

## Micromixing using planar curved channels

Arjun P. Sudarsan and Victor M. Ugaz  
Department of Chemical Engineering,  
Texas A&M University,  
3122 TAMU,  
College Station, TX 77843-3122  
USA

### Introduction

The inability to achieve passive mixing in planar microchannels continues to be a challenging problem in microfluidic technology. Micromixer design, however, has proven to be challenging due to the constraint of operating in a diffusion-dominated regime characterized by an unfavorable combination of low Reynolds numbers ( $Re = Vd/\nu \ll 100$ , where  $V$  is the flow velocity,  $d$  is the channel hydraulic diameter, and  $\nu$  is the fluid kinematic viscosity) and high Péclet numbers ( $Pe = Vd/D > 100$ , where  $D$  is the molecular diffusivity). Consequently, the characteristic downstream distances over which liquids must travel in order to become fully intermixed can be quite large ( $\Delta y_m \sim V \times d^2/D = Pe \times d$ ), often on the order of several cm. Recent work has shown that by patterning channel walls with grooved structures, transverse flows can be generated to chaotically mix fluids [1]. Other techniques involve flow lamination [2] where multiple interfaces between fluids are created to increase the overall interface area for diffusive mixing to take place. Although these techniques have made useful contributions, most of them induce additional complexities to device fabrication, as the final channel structure is three-dimensional and requires more than one lithography steps.

In this work, we show that planar curved channels can be used to mix fluids at length scales comparable to mixers from literature. As fluid is transported through a curvilinear channel, it experiences an interplay between inertial forces acting to direct its motion in the axial direction and centrifugal effects acting in the direction of the conduit's radius of curvature. The centrifugal effects establish a radial pressure gradient whose magnitude can become sufficient to generate a transverse secondary flow field superimposed on the bulk axial motion. The magnitude of the transverse secondary flow is characterized in terms of a dimensionless *Dean number* (**Error! Objects cannot be created from editing field codes.**) that expresses the ratio of inertial and centrifugal forces to viscous forces [3]. Here,  $Re$  is the Reynolds number ( $Re = Vd/\nu$ , where  $V$  is the flow velocity,  $d$  is the channel hydraulic diameter, and  $\nu$  is the fluid kinematic viscosity) and  $\delta$  is a geometric parameter characterizing the magnitude of the centrifugal effects (here, we define  $\delta = d/R$ ; where  $R$  is the radius of curvature of the flow path). The secondary flow field is characterized by a pair of counter-rotating vortices located symmetrically above and below the channel midplane.

This intrinsic rotational character of Dean flows can be harnessed in combination with a simple 2-D microchannel design to greatly enhance the interfacial area between species without the need to construct complex 3-D geometries. In our planar design, parallel liquid streams first travel through a curved segment that induces simultaneous 90° rotations in the upper and lower halves of the channel, after which the flow is split into multiple streams that continue along curved trajectories such that the flow in each individual stream experiences a second pair of 90° rotations. These successive rotation

steps transpose the position of each species such that alternating lamellae are formed when the streams are rejoined. Using this approach, split-and-recombine mixing can be performed in an easily fabricated 2-D microchannel geometry. We visualized this Dean flow mediated lamination process by performing confocal cross-sectional imaging experiments in a microchannel that is split into four parallel streams at a distance of 1.2 mm from the entrance and subsequently rejoined at a downstream distance of 4 mm (Fig. 1). At low flow rates, the secondary flow is not strong enough to induce a sufficient degree of rotation. At higher flow rates, however, the fluid species undergo a sequence of rotations such that upon rejoining, alternating lamellae of each species appear accompanied by a corresponding increase in interfacial area (see exit image sequence in Fig. 1).

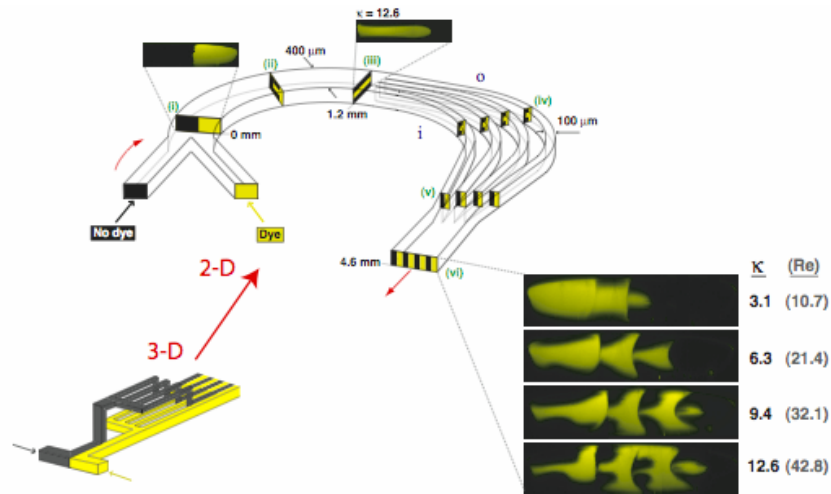


**Fig. 1.** Planar 2-D microchannel geometry capable of generating alternating lamellae of individual fluid species in a split-and-recombine arrangement (400  $\mu\text{m}$ -wide, 29  $\mu\text{m}$ -tall, 630  $\mu\text{m}$  radius of curvature,  $Re$  and  $\kappa$  computed based the 400  $\mu\text{m}$ -wide segment). Flow schematics are shown inside the channel, corresponding confocal images are shown outside.

We investigated additional alterations to curved 2-D microchannel geometries in order to further enhance mixing efficiency while minimally impacting flow conditions. Beyond a critical  $Re$ , fluid encountering a sudden increase in channel cross-sectional area undergoes local separation from the channel wall in response to the adverse pressure gradient resulting in the formation of a vortex pair located on either side of the entrance to the expansion. When these phenomena are coupled (Dean effects in the horizontal plane and expansion effects in the vertical plane), the action of these multiple vortices can be harnessed to greatly enhance the interfacial area available for interspecies diffusion (Fig 2A). This phenomena can be seen by direct visualization of colored dye streams in a microchannel geometry incorporating expansions from 100 to 500  $\mu\text{m}$  in width at flow rates corresponding to  $2.6 < Re < 51.6$  ( $0.7 < \kappa < 13.8$ ). The effectiveness of expansion vortices in promoting mixing is evident by constructing a curved serpentine microchannel incorporating abrupt expansions at periodic locations along the flow path and observing its effect on binding interactions between a fluorescent intercalating dye and double-stranded DNA (Fig. 2B). Fluorescence intensity in the microchannel increases and grows to occupy the entire cross section with increasing  $\kappa$ , indicating an

increased population of bound species. Cross-sectional confocal imaging of aqueous streams, one of which is fluorescently labeled, confirms that mixing is only enhanced above a critical flow rate at which the strength of both Dean and expansion vortices becomes significant (Fig. 2C).

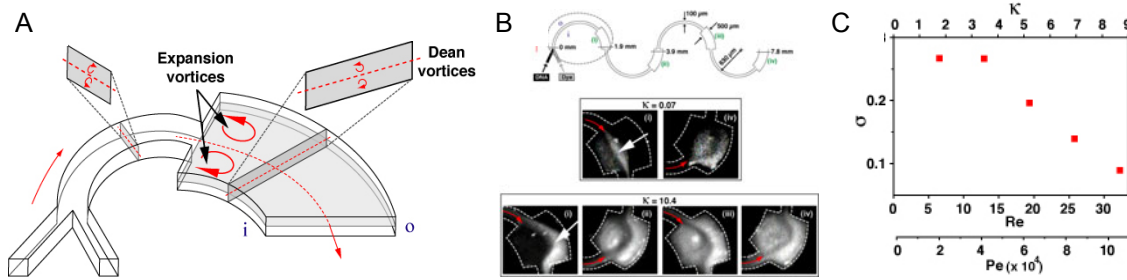


**Fig. 2.** (A) Schematic of a microchannel incorporating coupled transverse Dean vortex and expansion vortex phenomena in the vicinity of an abrupt increase from 100 to 500  $\mu\text{m}$  in width occurring over the last quarter of each semi-circular arc (29  $\mu\text{m}$  tall, 630  $\mu\text{m}$  radius of curvature,  $Re$ ,  $\kappa$  computed based on the 100  $\mu\text{m}$ -wide segment, “i” and “o” denote the inner and outer channel walls). (B) Binding enhancement between double-stranded DNA (calf thymus, 2.5  $\mu\text{g}/\text{mL}$ ) and an intercalating dye (ethidium bromide, 50  $\mu\text{g}/\text{mL}$ ) with increasing  $\kappa$  (dashed lines denote the microchannel walls). Red arrows indicate the flow direction, and white arrows indicate increased fluorescence above the background level of the unbound dye due to intercalation at the interface between streams. The binding interface is confined to the vicinity of the channel centerline at  $\kappa=0.07$ , but grows to occupy the entire channel cross-section at  $\kappa=10.4$ . (C) Plot of the standard deviation,  $\sigma$ , of fluorescence intensity over the channel cross-section at position (iv) computed from confocal imaging of two aqueous streams with one of them fluorescently labeled with Rhodamine 6G. A level of 80% mixing is achieved at the 7.8 mm downstream position for  $\kappa=8.6$ .

Finally, we show hybrid designs incorporating asymmetrically slanted barriers at specific locations in the curved flow path that are capable of effective mixing over a greatly expanded Reynolds number range than has been previously demonstrated.

## References

- [1] A. D. Stroock *et al.*, *Science* **295**, 647-651, (2002).
- [2] F. G. Bessoth *et al.*, *Commun.* **36**, 213-215, (1999).
- [3] S. A. Berger, L. Talbot, *Ann. Rev. Fluid Mech.* **15**, 461-512, (1983).